Supporting Information

Lotus-Inspired 3D Biomimetic Design toward Advanced Solar Steam Evaporator with Ultrahigh Efficiency and Remarkable Stability

Rong Zhang,[1,2‡] Bo Xiang,[1,2‡] Yating Wang,[1] Shaochun Tang,[1*] Xiangkang Meng[1]

[1] National Laboratory of Solid State Microstructures, Collaborative Innovation Center of Advanced Microstructures, Jiangsu Key Laboratory of Artificial Functional Materials, College of Engineering and Applied Sciences, Nanjing University, Nanjing 210093, P. R. China.

[2] College of Science, Nanjing Forestry University, Nanjing 210037, P. R. China.

‡ These authors contributed equally to this work.

*Corresponding author. Email: tangsc@nju.edu.cn

Figures

Fig. S1 Infrared reflection spectra of CP, CPZ and HCPZ.

Fig. S2 Schematics for the preparation process of PZ-precursor.

Fig. S3 SEM image of PZ**.**

Fig. S4 TEM images of CPZ.

Fig. S5 (a) N_2 adsorption-desorption isotherms of the hierarchical CPZ and PZ microtubes at 77 K and (b) corresponding pore size distribution calculated using the BJH method.

Fig. S6 EDS analysis of CPZ.

Fig. S7 High-resolution XPS spectra of CPZ.

Fig. S8 SEM image of CPZ.

Fig. S9 Schematics for the preparation process of HCPZ.

Fig. S10 (a-c) Photographs of solar-driven evaporation device for outdoor practical applications and the evaporation progress within one day. (d) Changes of humidity, temperature and solar flux in the daytime. The photos of device were recorded outside of the building of College of Engineering and Applied Sciences of Nanjing University on January 11th at Nanjing City, P. R. China (32°7'16"N, 118°57'19"E).

Fig. S11 A picture of solar-driven evaporation testing device.

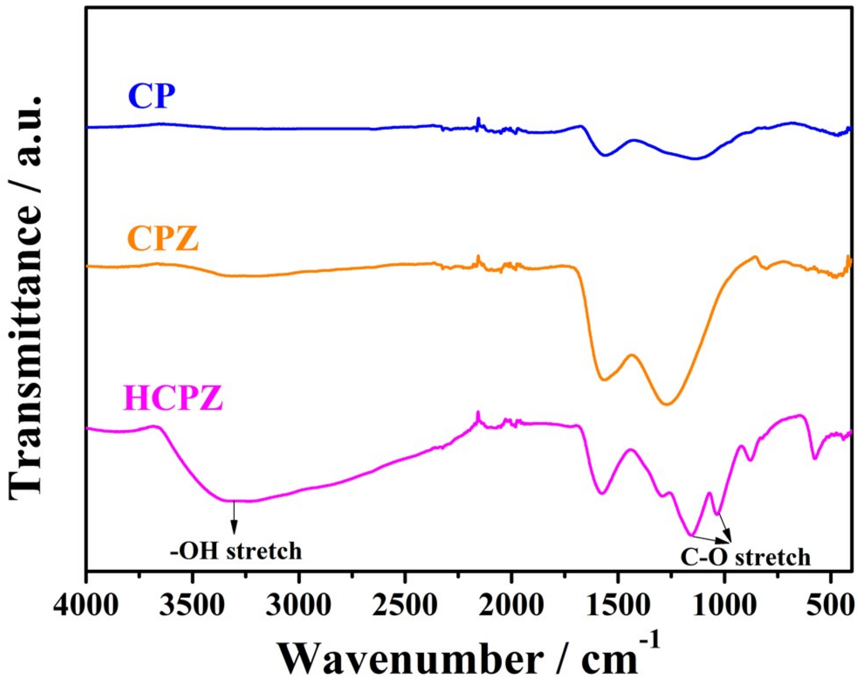

Fig. S1 Infrared reflection spectra of CP, CPZ and HCPZ.

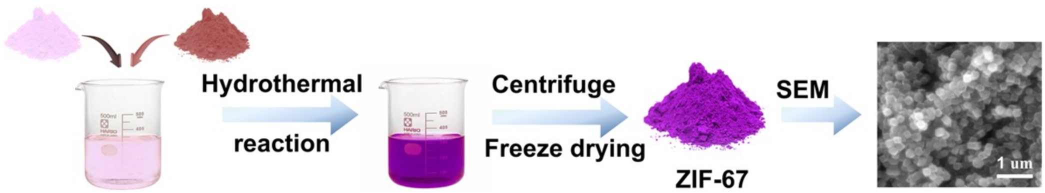

Fig. S2 Schematics for the preparation process of PZ-precursor.

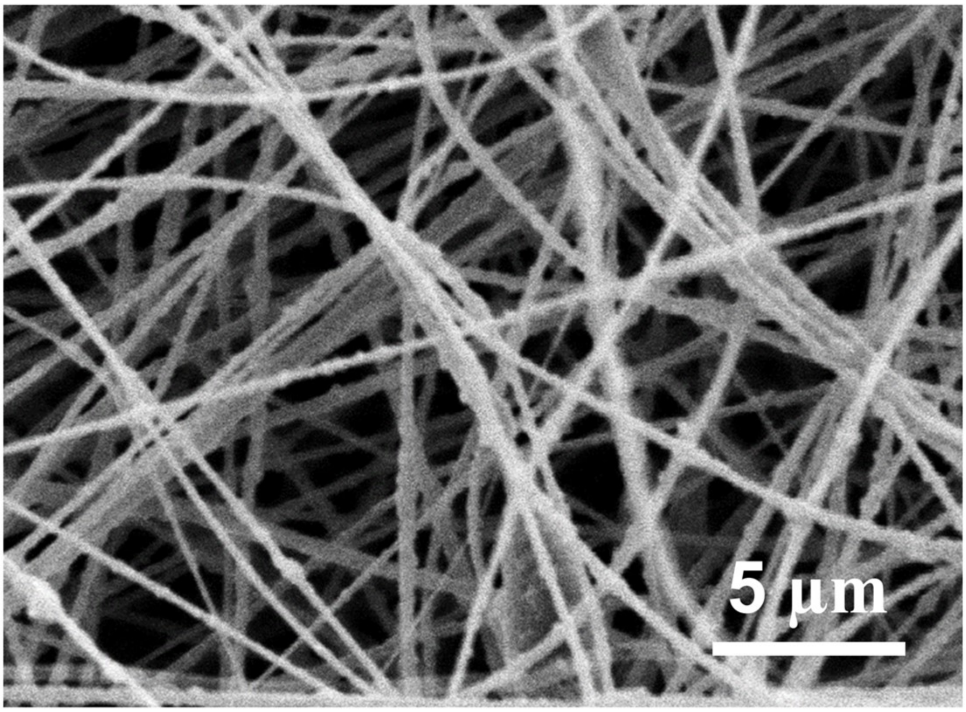

Fig. S3 SEM image of PZ**.**

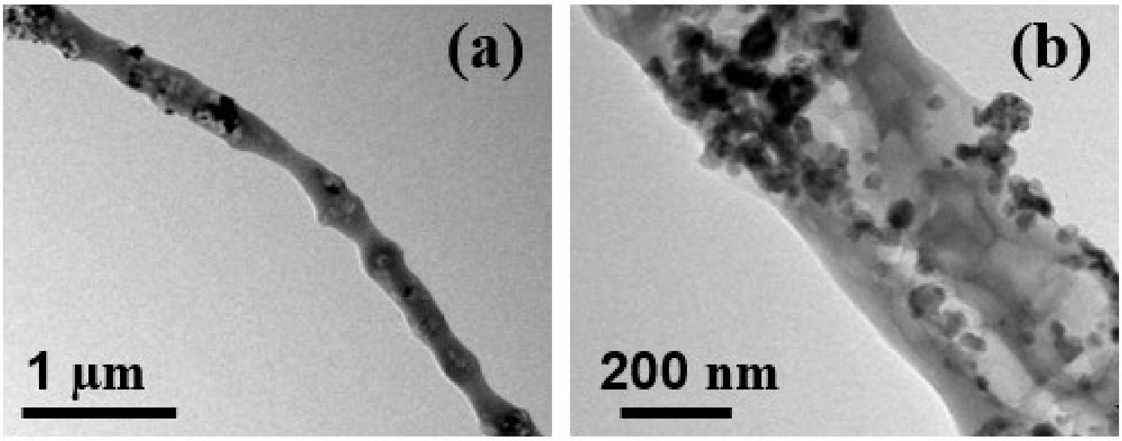

Fig. S4 TEM images of CPZ.

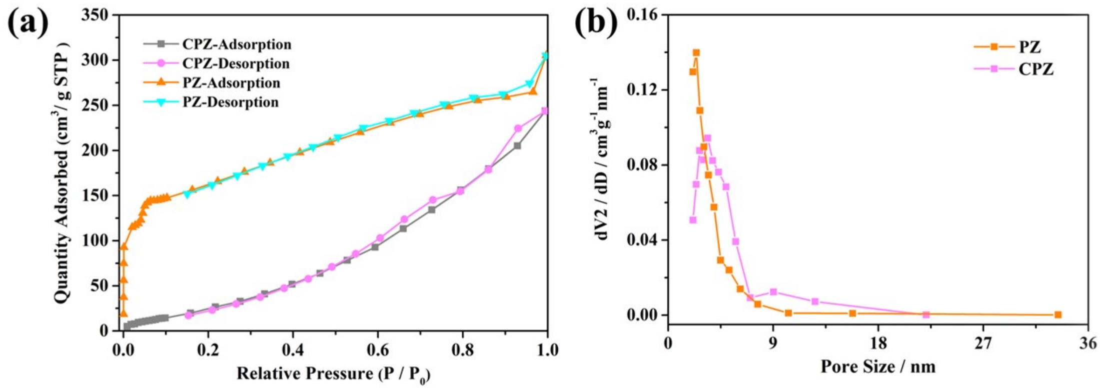

Fig. S5 (a) N_2 adsorption-desorption isotherms of the hierarchical CPZ and PZ microtubes at 77 K and (b) corresponding pore size distribution calculated using the BJH method.

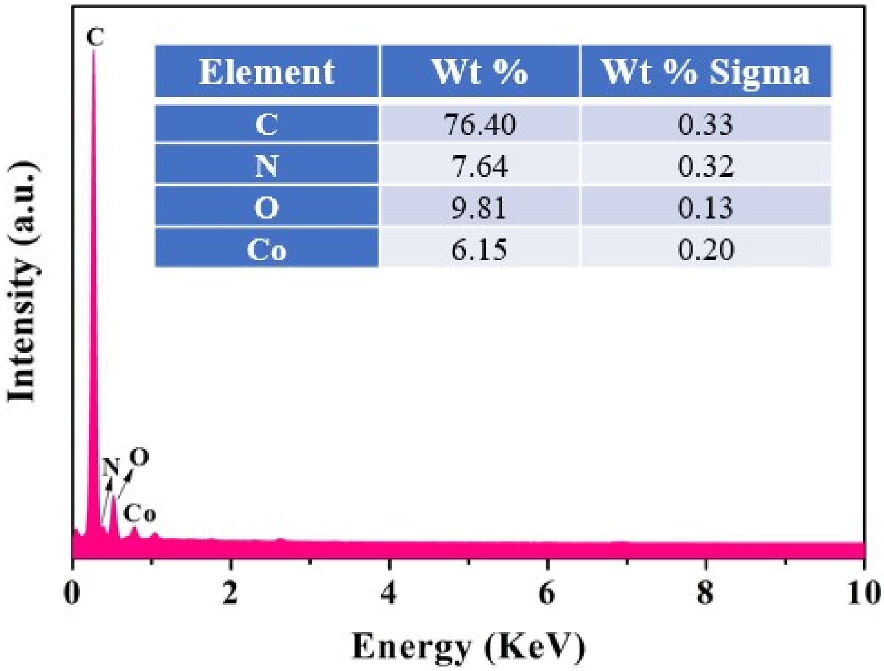

Element	Wt %	Wt % Sigma
C	76.40	0.33
N	7.64	0.32
O	9.81	0.13
Co	6.15	0.20

Fig. S6 EDS analysis of CPZ.

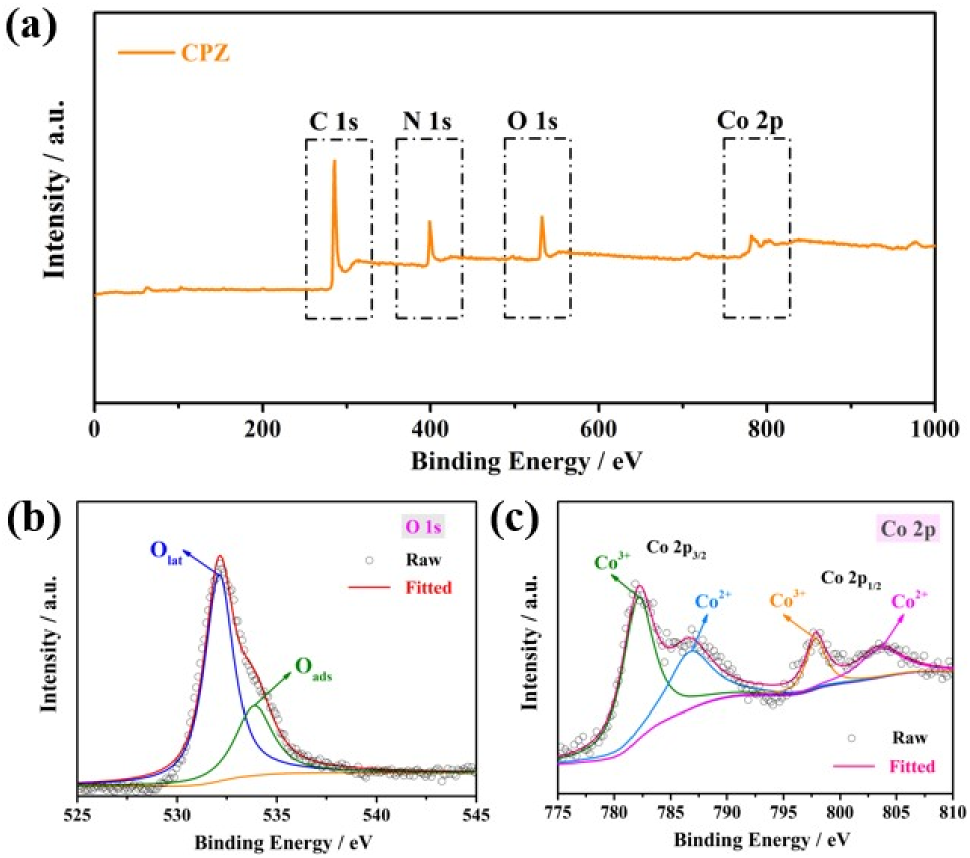

Fig. S7 High-resolution XPS spectra of CPZ.

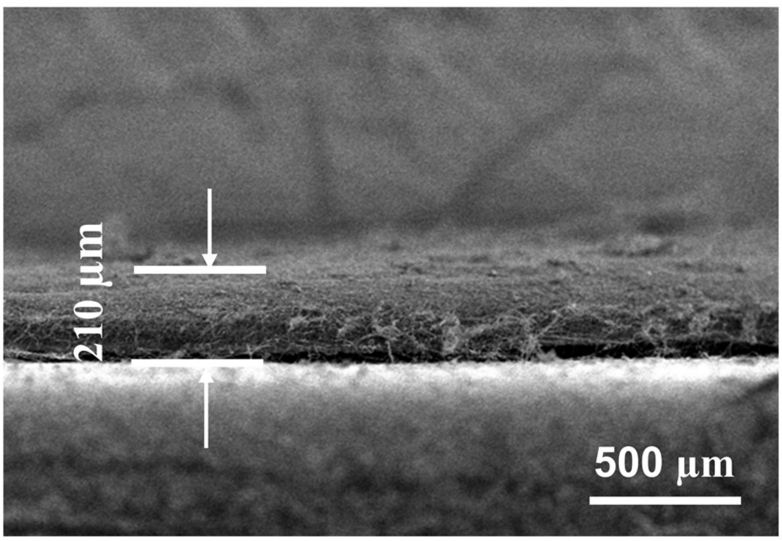

Fig. S8 SEM image of CPZ.

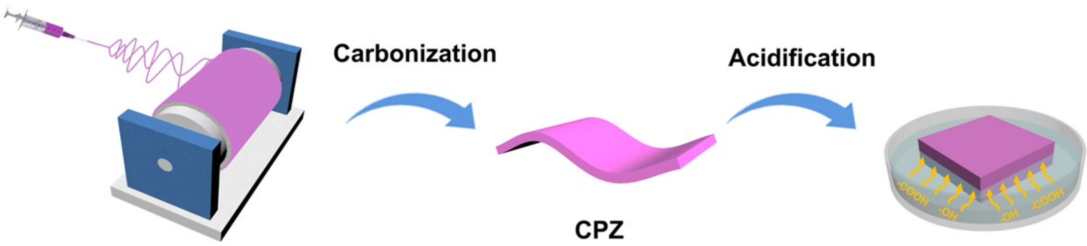

Fig. S9 Schematics for the preparation process of HCPZ.

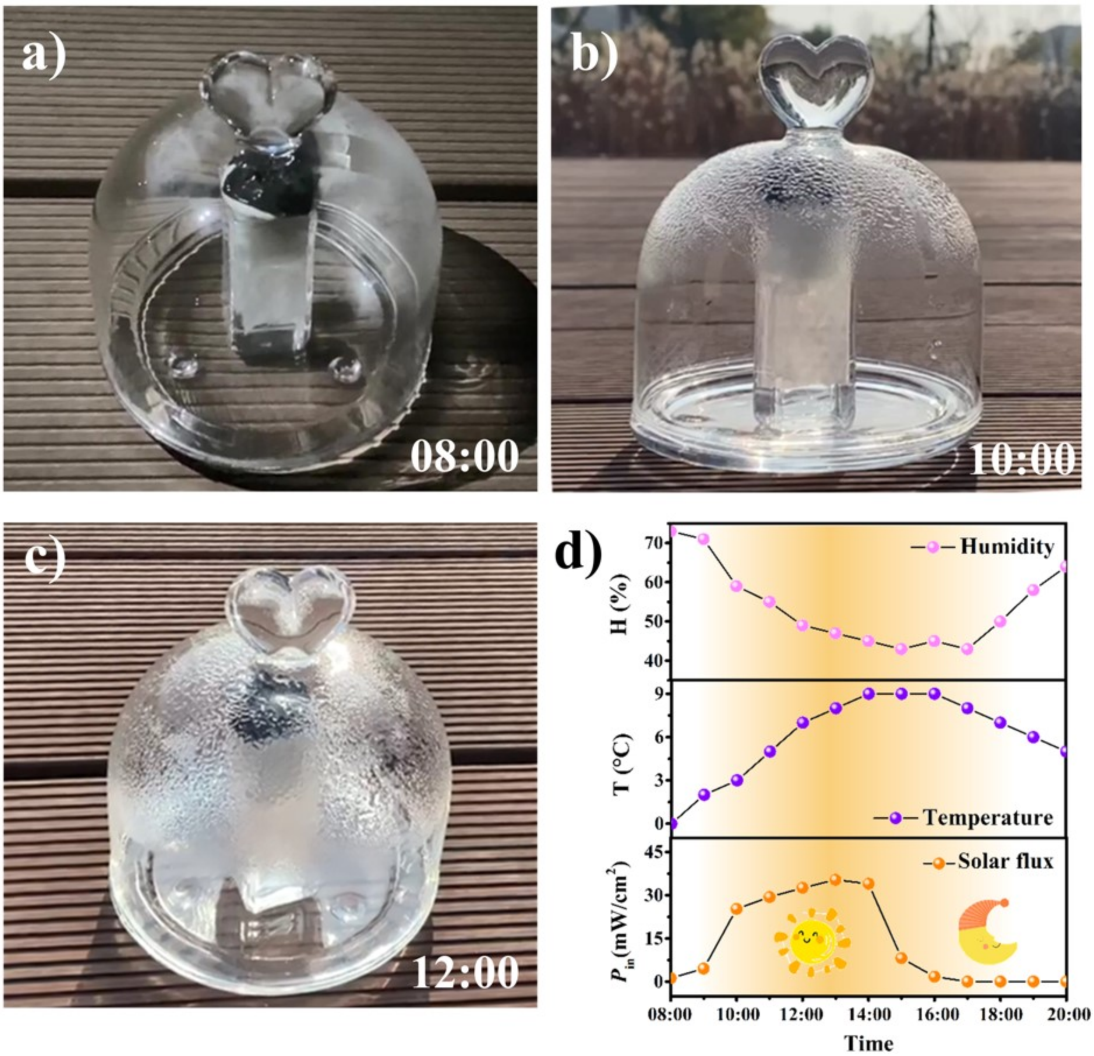

Fig. S10 (a-c) Photographs of solar-driven evaporation device for outdoor practical applications and the evaporation progress within 1 day. (d) Changes of humidity, temperature and solar flux in the daytime. The photos of device were recorded outside of the building of College of Engineering and Applied Sciences of Nanjing University on January 11th at Nanjing City, P. R. China (32°7'16"N, 118°57'19"E).

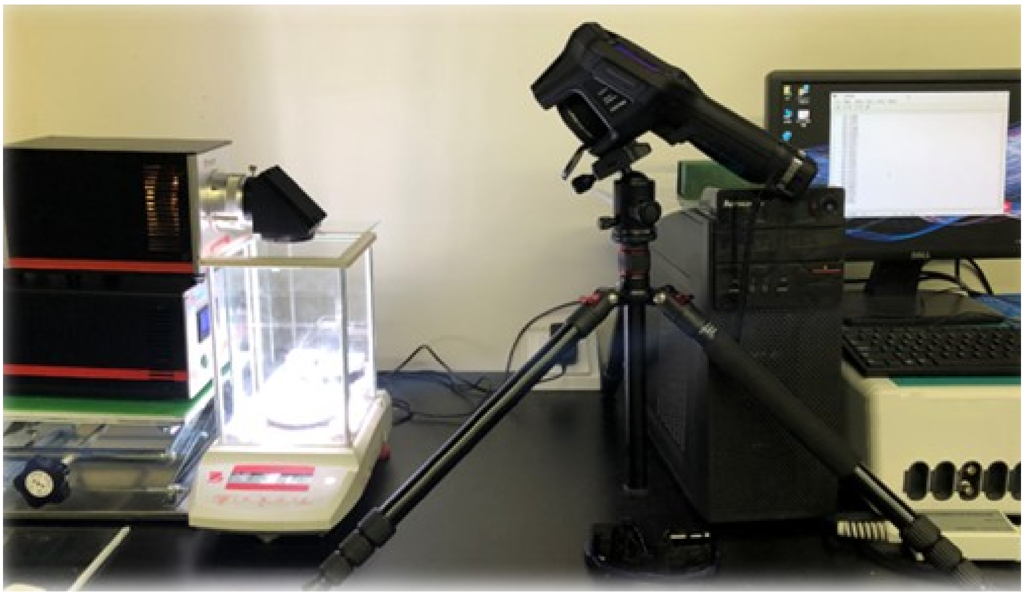

Fig. S11 A picture of solar-driven evaporation testing device.

Table S1. Comparison of solar steam generation performance of various solar absorbers under one sun irradiation (1 kW/m^2).

Solar absorbers	Evaporation rate (kg/m^2/h)	Efficiency (%)	Refs.
Plasmonic wood	1.0	65	1
ISWP	1.06	70	2
CB/PMMA-PAN	1.30	72	3
Carbonization wood	1.46	75	4
Carbonized mushrooms	1.48	78	5
Arched Bamboo	1.19	80	6
rGO-MWCNT film	1.22	80.4	7
PAN-CNT fabrics	1.44	81	8
MnO_2 deposited wood	1.22	81.4	9
HNG	3.2	84	10
3D-CG /GN	1.25	85.6	11
Carbonization melamine foams	1.27	87.3	12
Macroporous 3D MXene	1.41	88.7	13
Wood@AIP	1.42	90.8	14
rGO-WA	1.35	90.89	15
Multilayer PPy nanosheets	1.38	92.12	16
Ni/CNM	1.67	94.9	17
3D origami	1.59	100	18
3D Co_3O_4/MXene	1.89	130.4	19
3D cup shaped evaporator	2.04	140	20
Lotus-inspired 3D biomimetic evaporator	3.23	153.20	Our work

Calculations of the Heat Loss

The heat loss during the evaporation process is mainly caused by three aspects, including radiation, convection and conduction. The detailed calculation methods are as follows:

1) Radiation Loss

With the assistant of an emissometer (AE1/RD1, Devices & Services Company, America), the emittance of 3D-LBE can be obtained as 0.76 ($\pm$0.02). Then, the radiation loss can be calculated by Stefan-Boltzmann[21]:

$$\Phi = \varepsilon A\sigma(T_1^4 - T_2^4) \tag{S1}$$

where Φ represents the heat flux, ε is the emittance of the absorber (0.76), A is the surface area of the absorber (5.45 cm^2), σ is the Stefan-Boltzmann constant (5.67×10^{-8} W $m^{-2}\cdot K^{-4}$), T_1 is the average surface temperature of the evaporator (22.8 ºC under 1-sun illumination), and T_2 is the ambient temperature (25 ºC).

Therefore, based on Eq. S1, we can calculate that the radiation loss accounts for -1.09% (under 1-sun illumination) of all the irradiation energy (0.498 J s^{-1} for 1-sun illumination while the solar absorbance is 91.37%).

2) Convection Loss

The heat convection occurs between the solar absorber surface and the ambient environment. Then, the radiation loss can be calculated by Newton's law[21]:

$$Q = hA(T_1 - T_2) \tag{S2}$$

where Q denotes the heat, h is the convection heat transfer coefficient (according to an early report[22], the convection heat transfer coefficient is about 5 W m^{-2} K^{-1}), A is the surface area of the absorber (5.45 cm^2), T_1 is the average surface temperature of the absorber, and T_2 is the ambient temperature.

Therefore, based on Eq. S2, we can calculate that the radiation loss accounts for -1.20% (under 1-sun illumination) of all the irradiation energy.

3) Conduction Loss

Here, the conduction loss refers to the heat from absorber to bulk water. In order to calculate the conduction loss, the entire vaporization system was put in a Dewar container under 1-sun illumination. Then, the conduction loss can be calculated by the following equation[21]:

$$Q = Cm\Delta T \tag{S3}$$

where Q denotes the heat, C is the specific heat capacity of water (4.2 J g^{-1} K^{-1}), m is the water weight (25 g), and ΔT is the elevated water temperature within 3600 s (0.3 ºC under 1-sun illumination).

Therefore, based on Eq. S3, we can calculate that the radiation loss accounts for 1.76% (under 1-sun illumination) of all the irradiation energy. (Note: As the evaporation experiment proceeds the water weight is constantly decreasing. Therefore, the calculated radiation loss value is larger than the actual value.)

REFERENCES

1. M. Zhu, Y. Li, F. Chen, X. Zhu, J. Dai, Y. Li, Z. Yang, X. Yan, J. Song, Y. Wang, E. Hitz, W. Luo, M. Lu, B. Yang and L. Hu, *Adv Energy Mater*, 2018, **8**, 1701028.
2. F. Wang, N. Xu, W. Zhao, L. Zhou, P. Zhu, X. Wang, B. Zhu and J. Zhu, *Joule*, 2021, **5**, 1602-1612.
3. W. Xu, X. Hu, S. Zhuang, Y. Wang, X. Li, L. Zhou, S. Zhu and J. Zhu, *Adv Energy Mater*, 2018, **8**, 1702884.
4. Y. Kuang, C. Chen, S. He, E. M. Hitz, Y. Wang, W. Gan, R. Mi and L. Hu, *Adv Mater*, 2019, **31**, 1900498.
5. N. Xu, X. Hu, W. Xu, X. Li, L. Zhou, S. Zhu and J. Zhu, *Adv Mater*, 2017, **29**, 1606762.
6. Z. Li, C. Wang, T. Lei, H. Ma, J. Su, S. Ling and W. Wang, *Adv Sustain Syst*, 2019, **3**, 1800144.
7. Y. Wang, C. Wang, X. Song, S. K. Megarajan and H. Jiang, *J Mater Chem A*, 2018, **6**, 963-971.
8. B. Zhu, H. Kou, Z. Liu, Z. Wang, D. K. Macharia, M. Zhu, B. Wu, X. Liu and Z. Chen, *ACS Appl Mater Inter*, 2019, **11**, 35005-35014.
9. D. Li, D. Han, C. Guo and C. Huang, *ACS Appl Energ Mater*, 2021, **4**, 1752-1762.
10. F. Zhao, X. Zhou, Y. Shi, X. Qian, M. Alexander, X. Zhao, S. Mendez, R. Yang, L. Qu and G. Yu, *Nat Nanotechnol*, 2018, **13**, 489-495.
11. Y. Li, T. Gao, Z. Yang, C. Chen, W. Luo, J. Song, E. Hitz, C. Jia, Y. Zhou, B. Liu, B. Yang and L. Hu, *Adv Mater*, 2017, **29**, 1700981.
12. X. Lin, J. Chen, Z. Yuan, M. Yang, G. Chen, D. Yu, M. Zhang, W. Hong and X. Chen, *J Mater Chem A*, 2018, **6**, 4642-4648.
13. X. Zhao, X. Zha, J. Pu, L. Bai, R. Bao, Z. Liu, M. Yang and W. Yang, *J Mater*

Chem A, 2019, **7**, 10446-10455.
14. T. Chen, Z. Wu, Z. Liu, J. T. Aladejana, X. A. Wang, M. Niu, Q. Wei and Y. Xie, *ACS Appl Mater Inter*, 2020, **12**, 19511-19518.
15. W. Chao, X. Sun, Y. Li, G. Cao, R. Wang, C. Wang and S. Ho, *ACS Appl Mater Inter*, 2020, **12**, 22387-22397.
16. X. Wang, Q. Liu, S. Wu, B. Xu and H. Xu, *Adv Mater*, 2019, **31**, 1807716.
17. C. Song, L. Hao, B. Zhang, Z. Dong, Q. Tang, J. Min, Q. Zhao, R. Niu, J. Gong and T. Tang, *Sci China Mater*, 2020, **63**, 779-793.
18. S. Hong, Y. Shi, R. Li, C. Zhang, Y. Jin and P. Wang, *ACS Appl Mater Inter*, 2018, **10**, 28517-28524.
19. Y. Lu, D. Fan, H. Xu, H. Min, C. Lu, Z. Lin and X. Yang, *Sol RRL*, 2020, **4**, 2000232.
20. Y. Shi, R. Li, Y. Jin, S. Zhuo, L. Shi, J. Chang, S. Hong, K. Ng and P. Wang, *Joule*, 2018, **2**, 1171-1186.
21. X. Li, W. Xu, M. Tang, L. Zhou, B. Zhu, S. Zhu and J. Zhu, *Proc Natl Acad Sci U S A*, 2016, **113**, 13953-13958.
22. H. Ghasemi, G. Ni, A. M. Marconnet, J. Loomis, S. Yerci, N. Miljkovic and G. Chen, *Nat Commun*, 2014, **5**, 5449.